J. Fluid Mech. (1967), *vol.* 27, *part* 3, *pp.* 609–623
Printed in Great Britain

Transient convection in a porous medium

By J. W. ELDER

Department of Applied Mathematics and Theoretical Physics,
University of Cambridge

(Received 25 October 1965 and in revised form 5 July 1966)

Laboratory and numerical experiments on non-steady convective flows in a porous medium are reported. The main objective is to note the detailed comparison found between the time-dependent solutions and the time-like development of the iterative solutions of the steady equations originally pointed out by Garabedian (1956) and others.

Two flows are chosen for study. The first is the flow which develops when a blob of hot fluid is released at the base of a porous slab. The second is the flow which develops when a portion of the base of a porous slab is suddenly heated. The former flow is very simple and ideally suited for establishing the numerical scheme. The latter flow, however, produces several unexpected features. The gross features of the time development, when the motion is strongly non-linear, show an alternation between periods of slow gradual adjustment and periods of rapid change.

1. Introduction

As has been frequently pointed out (Garabedian 1956), the behaviour of the numerical solution of a system of steady elliptic equations by an iterative procedure develops in a time-like manner. Now in a typical problem with mesh spacing of order 1/30, the time-dependent problem can take of order 10^2 times as long to solve as the corresponding steady problem. If one is interested mainly in the gross features of the development of the flow, that is in the large eddies, it would be very convenient to solve the steady problem instead provided one could relate the number of iterations to the time. The demonstration that this is indeed possible and what one must sacrifice is a major task of this paper.

Free convection in a porous medium provides a convenient flow for this study. The numerical calculation is very straightforward and laboratory measurements made in a Hele-Shaw cell, which provides a two-dimensional analogue of a porous medium, are readily obtained for comparison with the numerical solutions. The numerical method for the iterative solution of the steady problem is that previously used by the author (1966*a*), while the time-dependent solution is obtained in essentially the same way except for the addition of the procedure for taking a step in time.

The problem is formulated and the numerical and experimental methods are described in §§ 2 and 3. Numerical and laboratory studies are then presented for: the rise of an isolated buoyant element (§ 4); and the sudden heating of a portion

of the base of the flow region (§§ 5 and 6). These studies allow verification of the numerical solutions and reveal details peculiar to the transient motions. Finally, in § 7, we discuss the suggestion of Garabedian.

2. The numerical method

2.1. *The system of equations*

Consider the motion of a fluid generated in a rectangular prism filled with a homogeneous porous material by heating the base. The field equations (Wooding 1957) for two-dimensional motion in dimensionless form† reduce to

$$\omega = A\theta_x, \quad \nabla^2\psi = \omega, \tag{1a,b}$$

$$F = \nabla^2\theta - \partial(\psi, \theta), \quad \partial\theta/\partial t = F. \tag{1c,d}$$

Note that the velocity $\mathbf{q} = (-\psi_z, \psi_x)$ and the vorticity $\boldsymbol{\omega} = -\hat{\jmath}\omega$ where $\hat{\jmath}$ is unit vector parallel to the y-axis. In (1): $A = krgH\Delta T/\nu\kappa_m$ is the Rayleigh number, ψ is the stream-function, θ is the temperature; $\partial(\psi, \theta)$ is the advection of heat, where we write ∂ for the Jacobian operator; and F is proportional to the rate at which a fluid element is gaining heat. These equations indicate that vorticity is generated by the horizontal gradient of the buoyancy forces and that heat is transferred both by conduction and advection. We observe that the system is non-linear solely because of the advection of heat, and time dependent solely through the thermal capacity of the medium. This is, therefore, one of the simplest time-dependent non-linear systems.

For the purpose of the discussion below we consider a typical problem in which the cavity of unit height and horizontal extent e is uniformly heated over a part of its lower surface of extent l, the other walls being held at zero temperature. Therefore, we chose initial conditions $\psi = \theta = 0$ everywhere for $t < 0$, and boundary conditions: $\psi = 0$ on the walls; $\theta = 1$ on $\frac{1}{2}(e-l) \leqslant x \leqslant \frac{1}{2}(e+l)$ and $z = 0$ for $t > 0$; and $\theta = 0$ elsewhere. For the study of the hot blob we chose $l/e \ll 1$ and also set $\theta = 0$ everywhere on the walls at a time $t_1 > 0$. We note that the above boundary conditions apply to impermeable conducting walls.

2.2. *Arrangement of calculations*

A suitable finite-difference representation of (1) is readily found by well-known methods (Fox 1962). The equations are solved as written in (1) in the order $(a, b, c, d, a, \ldots)$ for a chosen number of time steps. Except for the time step, the only point for comment is that the Poisson equation (1*b*) is solved by repeated application of Leibmann's extrapolated method with alternating directions of scan (Elder 1966*a*). In the present calculations, for each time step I have used eight applications of Leibmann's method. This is sufficient to obtain the new solution of (1*b*) to a precision of about 1 %.

† The notation follows Elder (1966*b*). The field variables have been made dimensionless by choosing units of length, temperature, velocity: the height of the box, H; the excess temperature of the heated region, ΔT; κ_m/H, where κ_m is the thermal diffusivity of the porous medium. A Cartesian co-ordinate frame O–XYZ, with its origin in the lower left-hand corner of the prism, has OX horizontal, OZ vertical such that motion is confined to planes y = const.

The integration of ($1d$) one step forward in time is performed in the simplest manner, i.e. we replace θ by $\theta + F\delta t$ where δt is the step in time. Now there are two well-known restrictions on δt. First, for a flow dominated by diffusion we require

$$\alpha \equiv \delta t/d^2 \leqslant \beta, \tag{2}$$

where β is a number and d is the mesh spacing. Numerical analysis shows that numerical instabilities develop (in two-dimensions) for $\beta = 0{\cdot}25$. Therefore, only

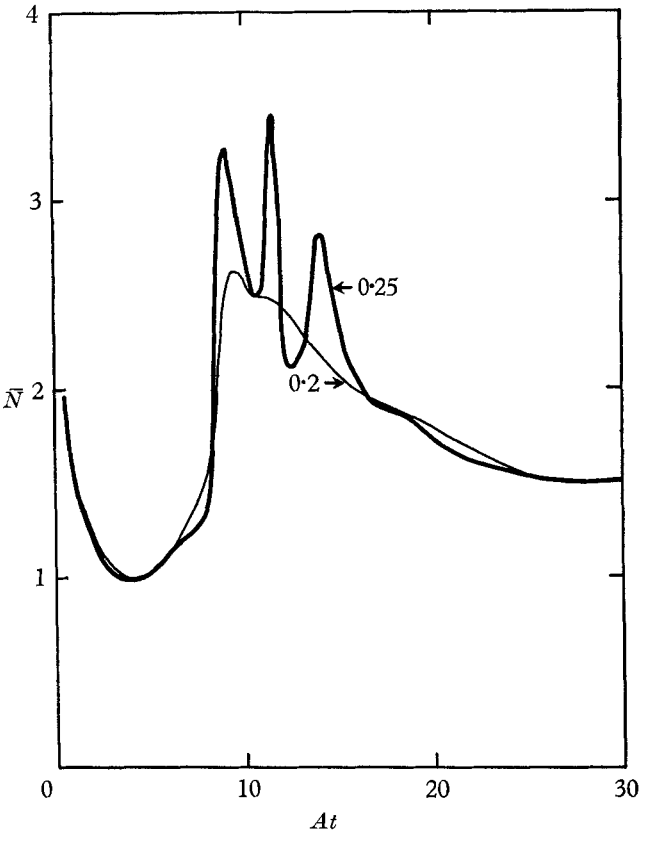

FIGURE 1. The role of α on the stability of the outer iteration. Mean Nusselt number $\bar{N}$ as a function of time t at Rayleigh number $A = 200$, mesh spacing $d = 1/10$ for the short-heater problems (PM 223 and 230).

small steps in time are permitted. This observation has led to considerable study of more elaborate time-step algorithms for which β can be much larger. These procedures are of no advantage here since at large Rayleigh numbers many of the phenomena proceed so fast, due to dominance of the advection, that using $\alpha = 0{\cdot}25$, would lose much of the detail and often lead to numerical instability. Such advective instabilities will certainly arise if the second restriction, noted by Courant, Friedrichs & Lewy (1928), is not satisfied. A fluid particle must not move a distance greater than the mesh spacing during a time increment. In the present calculations neither of these restrictions has been an inconvenience and the Courant, Friedrichs, Lewy condition has proved an excellent guide in choosing

δt. If we chose, for a given geometry and boundary conditions, values of d and δt just sufficient to avoid advective instabilities the computing time for flows dominated by advection is independent of the Rayleigh number.

2.3. *Stability of the numerical solutions*

The role of α in the stability of the outer iteration has been determined for the problems below. A typical result for the problem of sudden heating, obtained while the results of figures 4 and 6–8 below were determined, is shown in figure 1. The mean Nusselt number

$$\bar{N} = -\frac{1}{2e}\int_0^e [\theta_z(x, 0) + \theta_z(x, 1)]\, dx \tag{3}$$

has been found as a function of the time t for two values of α at a Rayleigh number A of 200. The curve for $\alpha = 0{\cdot}2$ is fairly smooth, the various bumps being identifiable with various details of the flow. The curve for $\alpha = 0{\cdot}25$ follows the other curve in broad detail but some of the bumps are greatly enhanced and extra bumps are present, for example here at $At = 14$. Further, during the interval $At = 8$ to 16, we find that $\theta > 1$ at some points within the cavity. Clearly this is not permissible and the solution must be rejected. Nevertheless, it is of interest to enquire into the nature of the region $\theta > 1$. It is seen from the temperature distribution to correspond to two blobs of hot fluid which very rapidly break off from each end of the lower heated region and rise vertically. Now this is close to what actually happens. Clearly therefore if we chose a value of α which is too large to follow important transient details of the motion the solution will be erroneous. It is interesting to note, however, that such a transient instability is not necessarily disastrous, since here the solution returns to the stable one.

3. The experimental method

All the experiments were performed in Hele-Shaw cells. These cells have already been used for a number of studies of flows in porous media and are well described elsewhere (e.g. Wooding 1963; Elder 1966*b*). If a viscous fluid flows between two sheets of insulating material held a small distance a apart, Hele-Shaw (1898) showed that the motion was closely similar to that in a porous-medium of permeability $\frac{1}{12}a^2$.

The apparatus was similar to those previously used by the author (Elder 1966*b*). The plate spacing was 4·0 mm, the depth of fluid 5 cm, the width of the cavity 20 cm. The fluid used was silicon oil MS 200/100 centistoke. Heat was supplied electrically. For the blob study the heated portion had a width of 0·5 cm and the remainder of the walls were made of Perspex. For the study of sudden heating the heated portion had a width of 10 cm, the upper surface was cooled by means of a thermostatic unit and the remainder of the walls were made of Perspex. The use of these partially insulating walls rather than conducting ones is a permissible convenience since the role of the boundary conditions on these walls is a minor one.

4. The rise of a hot blob

To establish the numerical scheme one needs for the initial study a simple flow which is reasonably well understood. The rise of a hot blob of fluid in a porous medium is the simplest example that comes to mind. Our task is simply to see if the numerical procedure works and the solutions are in reasonable agreement with laboratory experiment. Once this is established we are justified in proceeding to more elaborate problems.

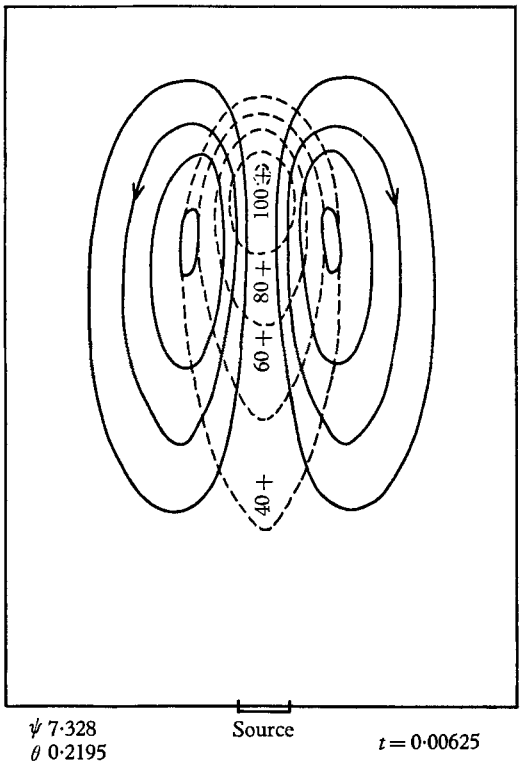

FIGURE 2. Isotherms (dotted lines) and streamlines (solid lines) for a hot blob. $A = 800$, $d = 1/40$, $\alpha = 0{\cdot}1$, $l = 0{\cdot}1$. The heater was left on for 40 time steps; the figure shows the flow after 100 time steps (PM 303). Note, in these figures the vertical scale is 5/3 of the horizontal scale.

Consider a blob of hot fluid produced by suddenly heating a portion of extent l of the lower surface of a slab of porous material for a time t_1. Clearly if we wish to study an isolated hot blob its dimension should be considerably smaller than those of the cavity. For this reason we choose $l \ll e$. Of course we could suddenly release a quantity of heat in the interior of the cavity but the method used here has some bearing on the flow discussed below. Also we observe that if t_1 is sufficiently small the blob never detaches itself from the lower surface. This is simply because if the heated region is small the motion is dominated by diffusion. We may estimate crudely a minimum (dimensionless) time t_1 for the release of a blob by requiring that the Rayleigh number based on the thickness of the heated

region near the source reaches the critical value of $4\pi^2$ (Lapwood 1948). The thickness of the heated layer is of order $2\sqrt{t}$ (Carslaw & Jaeger 1959, § 2.2). Hence the minimum time is

$$\min(t_1) \sim 400/A^2, \tag{4}$$

which corresponds to a minimum real time $400\kappa(\nu/krg\Delta T)^2$: a result independent of H, as it should be.

Figure 2 shows an example of a hot blob, obtained with $A = 800$, $t_1 = 0{\cdot}0025$ and $\alpha = 0{\cdot}1$ at time $t = 0{\cdot}00625$, when it has risen about half way up the cavity. We observe the localization of the isotherms, the pronounced gradient at the front of the blob and that the streamlines are much more extensive than the isotherms. At this stage the blob is fairly well isolated from the walls (the mean heat flux through the upper surface is $2{\cdot}89 \times 10^{-12}$) but is slowly decelerating. The maximum value of the stream function over the mesh has fallen from its maximum value of 11·94 (at time $t = 0{\cdot}0025$) to its present value of 7·328. By the time $t = 0{\cdot}01$ the blob will have begun to spread out on the upper surface.

Figure 2 can be compared with the experimental results of figure 3 (plate 1). Figure 3 was obtained in the following way. After some trial and error the heating current required to give $A = 800$ is determined. Also, we obtain the actual time from the time unit $H^2/\kappa_m = 2{\cdot}4 \times 10^4$ sec for $H = 5$ cm and 100 centistoke silicon oil. Hence, from the above dimensionless times we required the heater to be on for 60 sec and the photograph to be taken at 150 sec. The photograph shows that the blob is close to the predicted position. The agreement in time is quite good and suggests that the numerical scheme is valid. The agreement is not perfect, largely because the heater has a finite thermal capacity.

5. Continuous heating over a short length

Consider now the flow produced by heating the base of the layer from $t = 0$. Here we study the flow with $e = 4$, $l = 2$. A system of large horizontal extent will be studied in § 6.

Figure 4 shows the distributions of ψ and θ for the time interval $t = 0$ to 0·1 at a Rayleigh number of 400. At first the layer becomes heated as if it were a semi-infinite slab except close to the ends of the heater. The first motion is a set of eddies growing in this region. They advect heat away from the ends of the heater to produce a small bump in the isotherms. By the time 0·005 a small eddy of reverse circulation is associated with the end eddies. At time 0·01 these double eddies are well established and produce a rapidly rising column of hot fluid above the ends of the heater. During the interval 0·01 to 0·02 a further set of eddies grows near the ends and a rapid adjustment of the end eddies occurs. In addition, a small double eddy, rather similar to the blob studied in § 4, forms over the middle of the heater. This double eddy now grows rapidly and by the time 0·05 has reached its maximum growth. The end eddies have now merged into single large eddies. These large eddies continue to grow and by the time 0·1 have absorbed the double eddy. The temperature distribution follows a similar pattern.

These changes are very close to those observed in the laboratory. Even minor details such as the appearance and growth of the blobs and the wiggles in the

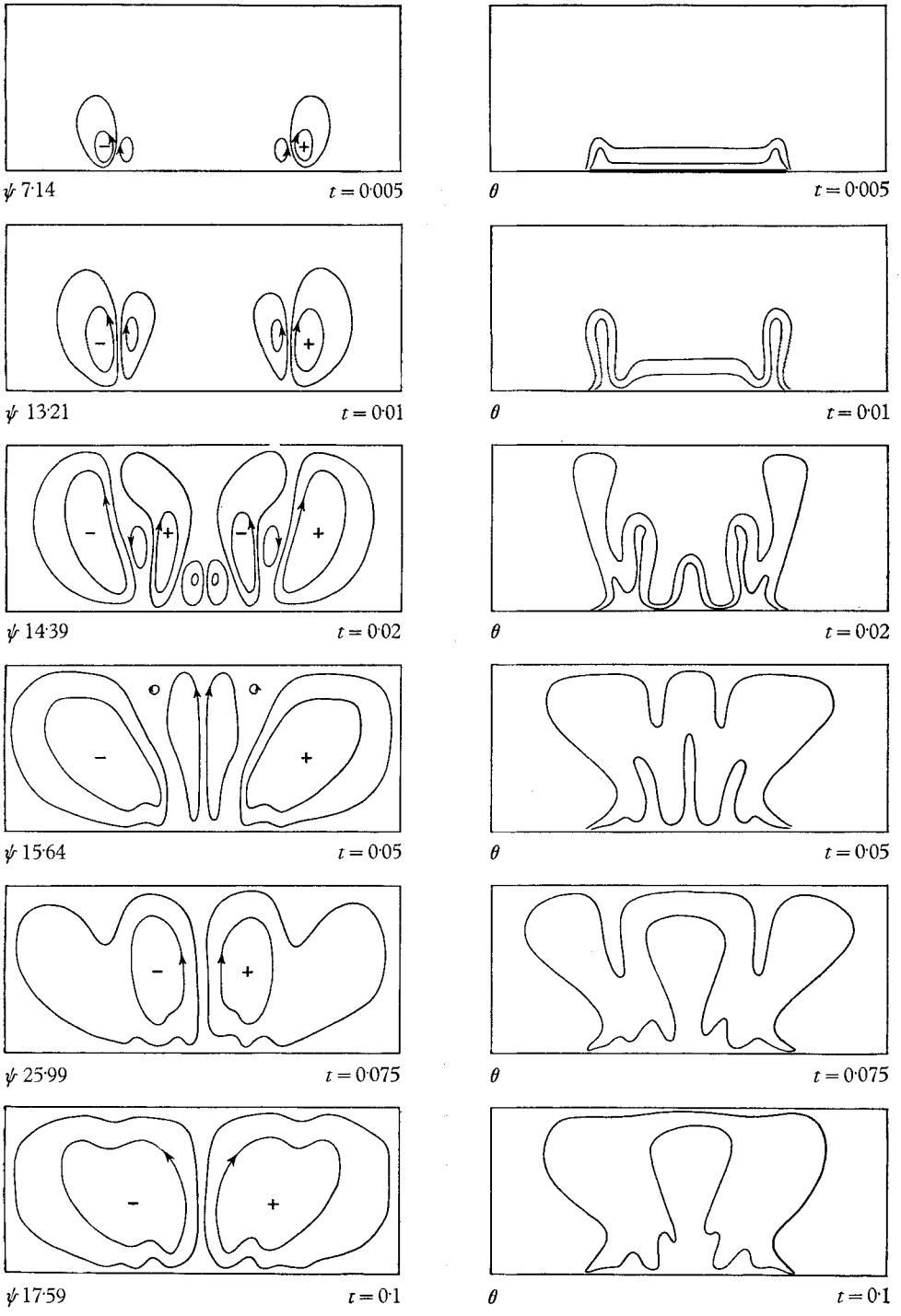

FIGURE 4. Stream-function and temperature distributions for the short-heater problem at various times: $A = 400$, $d = 1/20$, $e = 4$, $l = 2$, $\alpha = 0{\cdot}1$. The curves show 0·2 and 0·6 of the maximum value (PM 275).

streamlines above the heater are similar. Figure 5 (plate 2) shows two visualizations of the flow at $t = 0{\cdot}025$, $0{\cdot}05$. The agreement is sufficiently good to give considerable confidence in the numerical solution. Indeed, the numerical solution can now be used to reveal detailed limitations in the Hele-Shaw cell, but this matter need not concern us here.†

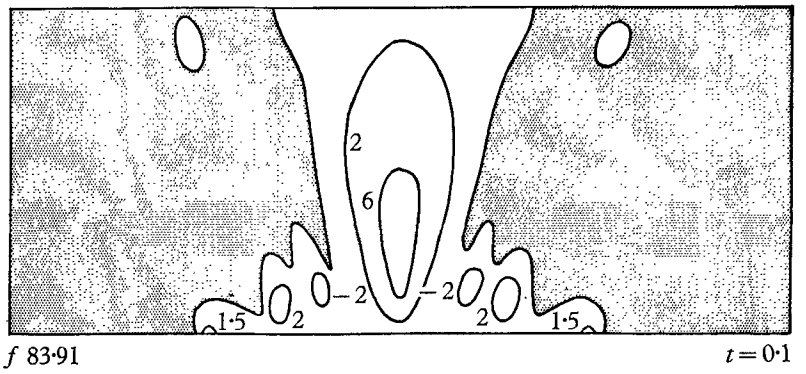

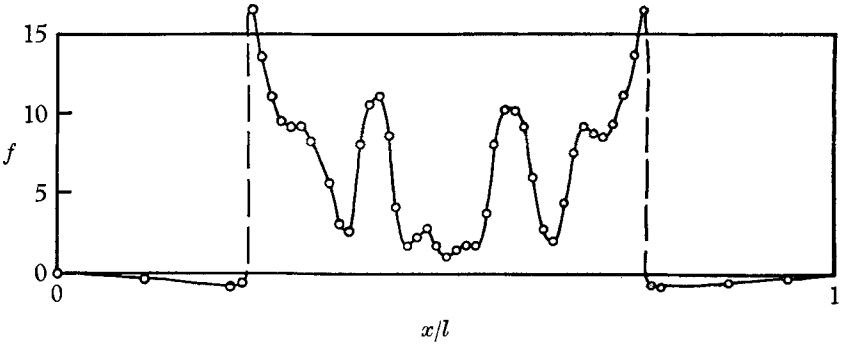

FIGURE 6. Vertical heat flux (5) for the flow of figure 4. The upper part of the figure shows the distribution of f, the lower part shows f on $z = 0$.

A quantity of considerable interest is the vertical heat flux

$$f = -\theta_z + \theta\psi_x, \tag{5}$$

the distribution of which is shown in figure 6 at $t = 0{\cdot}1$. The bulk of the heat is carried in the hot plume which rises above the centre of the heater. Heat is advected into the base of the plume through the thermal boundary layer near the heater. The small regions labelled 2 and -2 (i.e. $\pm 0{\cdot}2$ of the maximum value of f)

† The most noticeable difference is observed in the time interval $t = 0$–$0{\cdot}02$, especially if the apparatus has not been left standing for an hour or so. Small blob-like eddies appear almost immediately between the end cells. By the time $t = 0{\cdot}02$ these have been absorbed by the motions described above. Undoubtedly they arise from small residual disturbances, being predicted by the usual linear stability theory. They are readily simulated numerically and have been described in a discussion of thermal turbulence of geophysical interest (Elder 1966c).

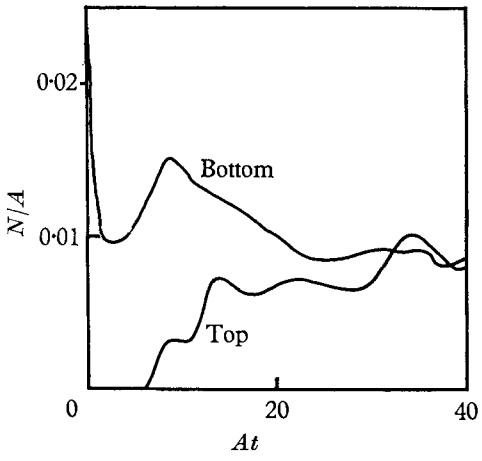

FIGURE 7. Nusselt number for the top and bottom surfaces as a function of time for the problem of figure 4.

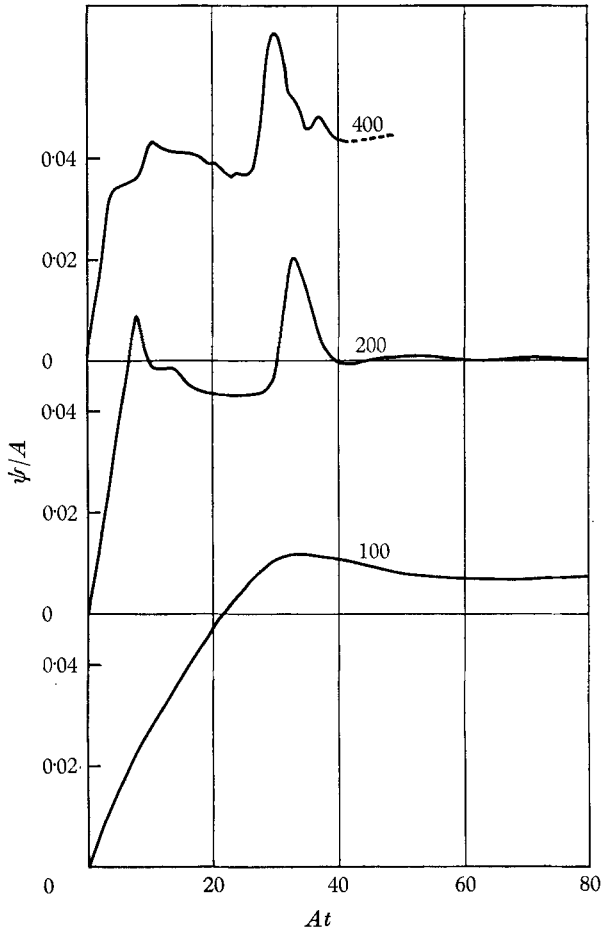

FIGURE 8. The maximum value of the stream function for the problem of figure 4 at A = 400, 200, 100 (PM 275, 224, 242).

correspond to small blobs which grow near the ends of the heater and become partially detached from the heater as they are advected through the heater boundary layer. Figure 6 also shows $f(x, 0)$ the rate at which heat enters the slab. We notice that $f(x, 0)$ is not quite symmetrical. This is due to the advection of the detached blobs being somewhat different on the two sides of the centre line.

The development of the system is summarized in figures 7 and 8. Figure 7 shows the mean Nusselt number on both $z = 0$ and 1 for the flow of figure 7. For a time less than $32/A$ the heat flow into the base of the slab exceeds that out of the layer so that heat is accumulating in the slab. Indeed there is no perceptible heat flow out of the slab till time $6/A$. The various wiggles reflect the growth and adjustment of the eddies in the slab. Beyond $At = 40$ only minor adjustments are necessary before equilibrium is established.

Figure 8 shows the maximum value of the stream function for the present problem with $A = 400$ and for $A = 100$ and 200. The most striking feature here is the great increase in detail and pronounced accelerations at the higher values of A.

In this study a useful simplification is to correlate variables of interest with a velocity unit proportional to A and a time unit proportional to $1/A$. Inspection of (1) shows that this would be strictly correct if the diffusion of heat could be ignored everywhere. Clearly this is not permissible near the boundaries, but as shown for example by figure 8 this is a good approximation. This is an important result for the extrapolation of these results to geophysical problems where the Rayleigh number can be of order 10^5. However, as figure 8 clearly indicates the extrapolated flow will lack much of the detail of the actual flow.

6. Continuous heating over a long length

For a horizontally infinite slab clearly the transient motions which occur immediately after $t = 0$ will be similar at every location. For a long but finite heater that this is not the case is shown in figure 9. This shows the distribution of ψ for a slab with $e = 10$, $l = 8$ at $A = 200$. The initial motion is very similar to that of figure 4 with the growth firstly of a pair of end-cells followed by the successive growth of a string of cells above the heater. The encroachment of these cells inward from the ends proceeds with a roughly constant horizontal velocity dX/dt, where X is the position in the fluid separating the regions of cellular motion from nearly stagnant fluid. We find

$$|dX/dt| \approx 30. \tag{6}$$

Following this encroachment there is a long period of gradual adjustment, till finally at this rather small Rayleigh number the flow is extremely symmetrical.

The gross features of the flow are shown in figure 10, which presents the mean Nusselt number (3) and the maximum value of the stream function. The remarkable feature of these curves, particularly for $\overline{N}$, is the marked variation between periods of rapid change and gradual change. We can identify the places where $\partial \overline{N}/\partial t$ is large and ψ has a maximum with the birth of a new pair of eddies. The author (1966*b*) has already suggested as a result of some laboratory studies that

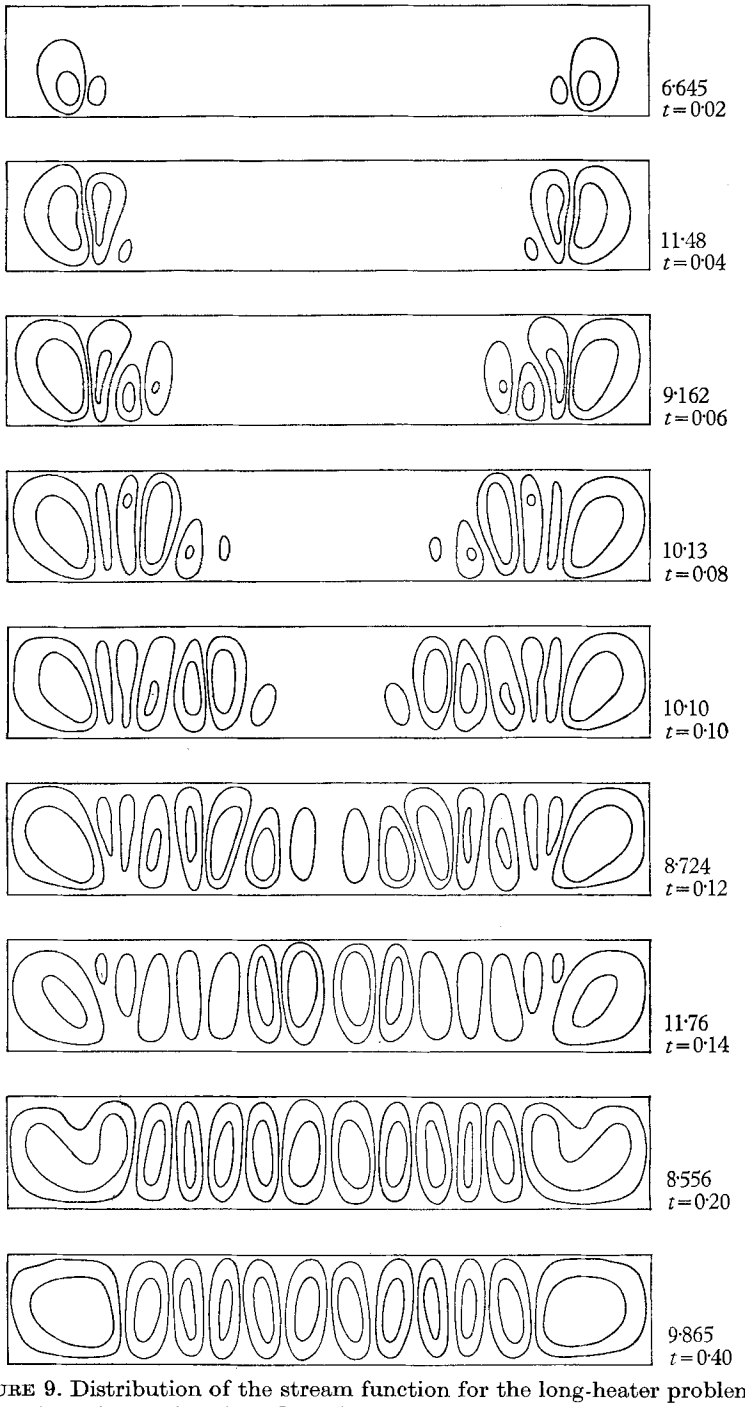

FIGURE 9. Distribution of the stream function for the long-heater problem at various times: $A = 200$, $d = 1/10$, $e = 10$, $l = 8$, $\alpha = 0·2$ (PM 225).

such phenomena exist and that they can provide an alternative explanation to that given by Malkus (1954) for his intriguing observations of breaks in the experimentally determined $\bar{N}(t)$ in an apparatus which was cooling down. The

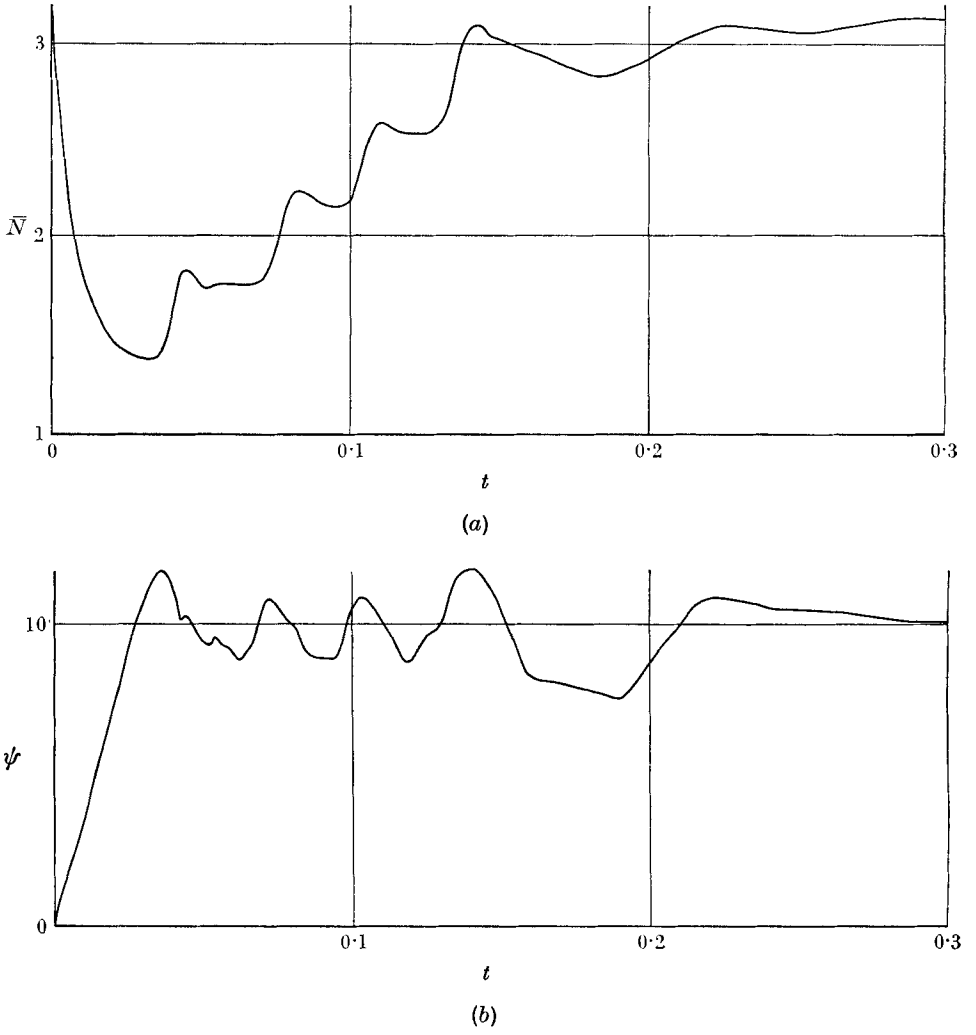

FIGURE 10. (*a*) The Nusselt number and (*b*) the maximum value of the stream function for the problem of figure 9.

increments in the curve of $\bar{N}$ in figure 10 are nearly equal, corresponding to a change.

$$\Delta N \approx 0{\cdot}4. \tag{7}$$

This is not surprising, since each new cell can be expected to transport an equal increment of heat.

7. On the time-like behaviour of the iterative solution of the steady problem

Since we can now solve both the time-dependent and the steady problems we can investigate in detail the suggestion of Garabedian (1956) and others. Our task is to relate the number of outer iterations s of the steady equations to the time t and see to what extent the details of the two solutions are related. The following examples are typical of this relationship.

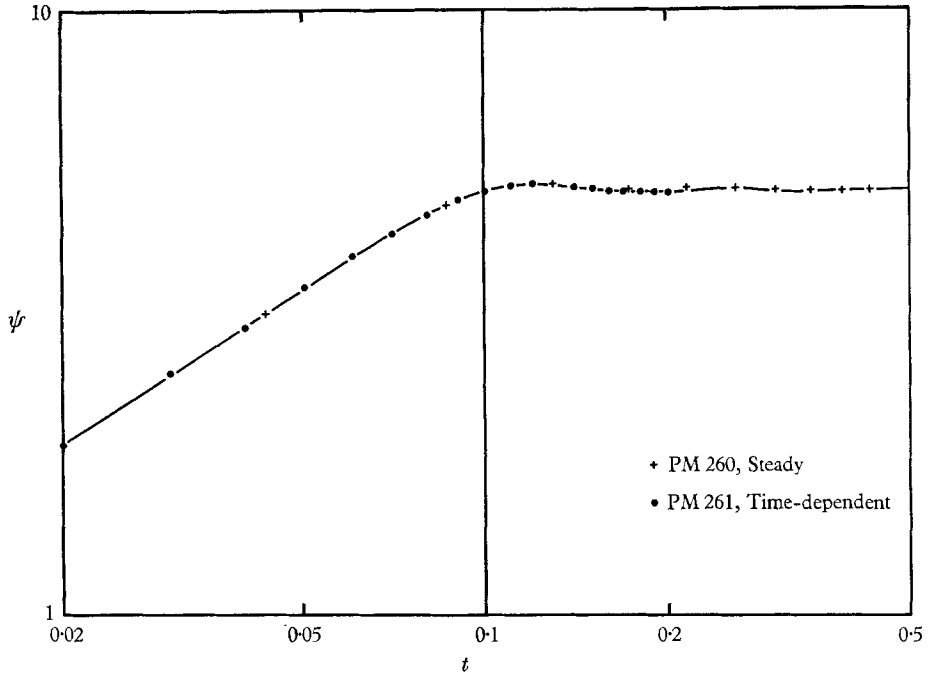

FIGURE 11. Comparison of the maximum value of the stream function in the short-heater problem for the solutions of the steady and the time-dependent problem. $A = 80, d = 1/10$.

Figure 11 presents solutions for the short-heater problem of § 5 at a Rayleigh number of 80. The maximum value of the stream function is shown as a function of t and of s, where s has been related to the time by

$$t = 4{\cdot}33d^2s. \tag{8}$$

Numerous tests show that for the same event sd^2 is a constant as we change d, and the coefficient 4·33 is chosen so that the two sets of data agree as much as possible. As can be seen the fit is very good; discrepancies are less than 1 %.

Inspection of the stream function distributions does, however, reveal considerable differences between the two solutions. An example of this is shown in figure 12 which gives solutions for the long-heater problem of § 6 at a Rayleigh number of 80. We find an identical relation (8) between t and s but the distributions are shown at the nearest corresponding values. (Strictly we should show the time-dependent solutions at times 0·0433, 0·0866, etc.) The broad features

of the development are similar, including the nearly uniform advance of the string of eddies, but the eddies of the steady problem are somewhat larger and make their first appearance a little later. In addition the final solutions have 10 Rayleigh cells for the time-dependent problem and 6 for the steady problem. This result is of considerable interest since it demonstrates the non-uniqueness

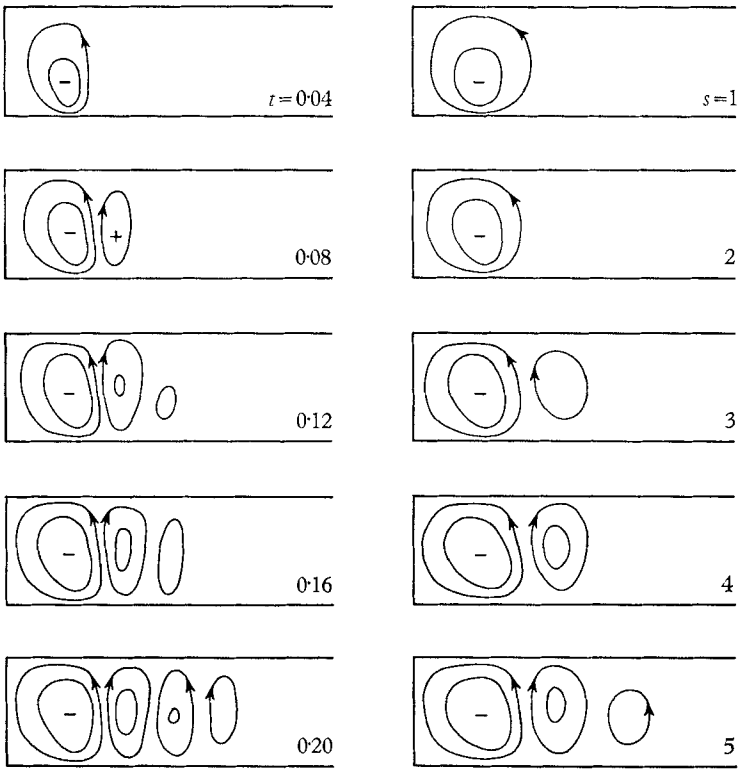

(*a*) Time-dependent (PM 221) (*b*) Steady (PM 262)

FIGURE 12. Comparison of the stream function in the long-heater problem for the steady and the time-dependent solutions. $A = 80$, $d = 1/10$. Only the left-hand half of the flow is shown.

in such systems. As well as the boundary conditions, one must specify the path the system has followed in order to specify the final solution (cf. Elder 1966*b*, § 5).

Some features of the time-dependent problem do not appear in the steady problem. In the problems studied so far, these features have been the small eddies, such as the blobs which rise above the heater in figure 4 at time 0·02. The steady solution is restricted to the large eddies, that is those motions which extend across the narrowest dimension of the cavity.

This simple study suggests that much useful information is available by judicious use of the steady solution by regarding s as a time. Clearly the coefficient 4·33 in (8) will depend somewhat on the problem and very much on the arrangement of the outer iteration. However, where the time-dependent solution is available it is a simple matter to find the appropriate value. On the other hand,

if the time-dependent solution is not available a crude estimate (within a factor of 2 or so) can be obtained by the following device, noted in Elder (1966*b*, § 4.2). Obtain the steady solution with $A = 0$, using a set of boundary conditions for which the purely conductive solution is known. We observe that the fields decay exponentially, as is to be expected (Carslaw & Jaeger 1959), e.g. a slab cools with a time constant of $1/\pi^2$. From the steady solution one readily finds the corresponding number of iterations s and hence the corresponding time. A very convenient and economical method for problems which have a steady or nearly steady state is to solve the time-dependent problem for the time interval in which the most rapid changes occur then use this solution as the test function for the steady equations.

I wish to acknowledge my debt to the members of the University of California, San Diego, Computing Centre. This work was supported by a National Science Foundation Grant GP-2414 and an Office of Naval Research Contract Nonr-2216. The manuscript was written while the author was supported by the British Admiralty.

REFERENCES

CARSLAW, H. S. & JAEGER, J. C. 1959 *Conduction of Heat in Solids.* Oxford: Clarendon Press.

COURANT, R., FRIEDRICHS, K. O. & LEWY, H. 1928 *Math. Ann.* **100**, 32.

ELDER, J. W. 1966*a* *J. Fluid Mech.* **24**, 823.

ELDER, J. W. 1966*b* *J. Fluid Mech.* **27**, 29.

ELDER, J. W. 1966*c* In: *The Mantles of the Earth and the Terrestrial Planets* (ed. S. K. Runcorn). New York: Wiley. (in the Press).

FOX, L. 1962 *Numerical Solutions of Ordinary and Partial Differential Equations.* London: Pergamon Press.

GARABEDIAN, P. R. 1956 *Math. Tables Aids Comput.* **10**, 183.

HELE-SHAW, H. S. J. 1898 *Trans. Inst. Nav. Arch.* **40**, 21.

LAPWOOD, E. R. 1948 *Proc. Camb. Phil. Soc.* **44**, 508.

MALKUS, W. V. R. 1954 *Proc. Roy. Soc.* A, **225**, 185.

WOODING, R. A. 1957 *J. Fluid Mech.* **2**, 273.

WOODING, R. A. 1963 *J. Fluid Mech.* **15**, 527.